

## Study of the Survival Probability and the Phase Diagram of the Electronic Frenkel-Kontorova Model

Bambi Hu<sup>1,2</sup> and Lei Yang<sup>1</sup>

<sup>1</sup>*Department of Physics, Centre for Nonlinear Studies,  
and The Beijing-Hong Kong-Singapore Joint Centre for Nonlinear and Complex Systems (Hong Kong),  
Hong Kong Baptist University, Hong Kong, China*

<sup>2</sup>*Department of Physics, University of Houston, Houston, Texas 77204-5005, U.S.A*

(Dated: February 4, 2005)

Electron transport in the Frenkel-Kontorova (FK) model is studied. The survival probability and, in particular, the dependence of the survival probability on the system size, is investigated. Based on these results, we obtain an approximate phase diagram of the FK model. The FK model is either Harper-like or Fibonacci-like, and there is a critical point separating these two states. It seems that this point corresponds to the breaking of analyticity transition critical point in the classical FK model.

Much effort has been devoted to the study of electron transport in 1D tight-binding models such as the disordered model, the Harper model, the Fibonacci chain and the Frenkel-Kontorova (FK) model. The Schrödinger equation describing these models is given by:

$$i \frac{d\psi_n(t)}{dt} = \psi_{n+1}(t) + \psi_{n-1}(t) + V_n \psi_n(t), \quad (1)$$

where  $\psi_n(t)$  is the wave function at the  $n$ th site. The nearest-neighbor hopping integral is set to 1.  $V_n$  is the external potential defining different models. For the Harper model [1],  $V_n = \lambda \cos(2\pi\sigma n)$ ; the Fibonacci model [2],  $V_n = abaababa\dots$  ( $\lambda = \frac{a}{b} - 1$ ); the FK model [3],  $V_n = \lambda \cos(x_n)$ , where  $x_n$  is the configuration of an incommensurate ground state. The electron transport behavior is determined by the external potential, whose periodicity and strength are two important parameters. These models exhibit a variety of behaviors such as ballistic motion, diffusion, and localization. Various quantities have been introduced to characterize the dynamics of a wave packet, for example, the variance [4], the front shape [5], the temporal correlation functions [6], and the survival probability [7]. The survival probability is an important tool to investigate a wave packet localized initially inside an open system for classical [8] and quantum systems [9]. Recently it has been applied to the Harper model and the Fibonacci model [7]. In this paper, the survival probability and, in particular, the dependence of the survival probability on the system size in the electronic FK model will be investigated.

The equation of motion of the electronic FK model is described by

$$\begin{aligned} i \frac{d\psi_n(t)}{dt} &= \psi_{n+1}(t) + \psi_{n-1}(t) + \lambda \cos(\pi x_n) \psi_n(t) \\ &= \sum_{m=n-1}^{n+1} H_{n,m} \psi_m(t). \end{aligned} \quad (2)$$

$\lambda$  is the strength of the external potential and  $H_{nm}$  a real symmetric three band matrix.  $x_n$  is determined by the ground state of the corresponding classical FK model:

$$H = \sum_n \frac{1}{2} (x_{n+1} - x_n - l_0)^2 + KV(x_n), \quad (3)$$

where  $l_0$  is the natural length of the spring,  $V(x_n) = \frac{1}{2}(1 - \cos(\frac{\pi x_n}{a}))$ ,  $a$  the periodicity, and  $K$  the strength of the external potential. Here  $l_0 = 2.0$ ,  $a = \frac{(\sqrt{5}-1)}{2}$ .

The numerical simulation proceeds as follow: (1) The time-dependent Schrödinger equation is integrated numerically by using a Cayley scheme [10]. (2) The initial wave function at one end of the boundaries is  $\psi_n(t=0) = \delta_{n,1}$ . (3) Attach 20 additional sites at the ends when the boundary  $\psi_n(t)$  is larger than  $10^{-14}$ . Eq. (2) then becomes

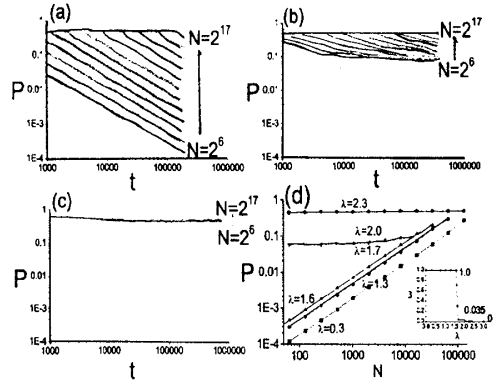


FIG. 1: Log-log plot of the survival probability  $P(t)$  at  $K = 0.15$  and various  $\lambda$  (a)  $\lambda = 1.3$ ; (b)  $\lambda = 2.2$ ; (c)  $\lambda = 2.3$ . In Fig. 1(d),  $P(N) \sim N^\beta$  for different  $\lambda$  at time  $t \sim 2 \times 10^5$ . The inset of Fig. 1(d) shows  $\beta(\lambda)$ .

$$\left(1 + \frac{1}{2}iH\delta t\right)\psi(t + \delta t) = \left(1 - \frac{1}{2}iH\delta t\right)\psi(t). \quad (4)$$

The Cayley scheme is accurate to second-order in time and it is unitary. Moreover, it's stable for the time-dependent Schrödinger equation. In this paper, we use a time step  $\delta t = 0.1$ , which is comparable to  $\delta t \sim 0.0005$  in the fourth-order Runge-Kutta method. Thus a faster simulation speed can be used to study the long-time dynamical behavior. The survival probability  $P$  is defined as

$$P(t) = \sum_{n=1}^N \psi_n^2(t), \quad (5)$$

where  $N$  is the size of an open system. In the paper,  $N = 2^i$  ( $i = 6 \dots 17$ ),  $K \in [0, 0.4]$ , and  $\lambda \in [0, 10]$ .

The simulation results are reported in Figs. 1 and 2 for two typical cases:  $K = 0.15$  and  $0.3$ , respectively. Figs. 1(a) - (c) show the survival probability  $P(t)$  for  $K = 0.15$ . In Fig. 1(a),  $\lambda = 1.3$ , the curves  $P(t)$  are parallel lines and show the power-law behavior  $P(t) \sim t^{-1}$  for all system sizes. So the system is in a purely ballistic state. In Fig. 1(b),  $\lambda = 2.1$ , the curves  $P(t)$  converge to a line which is parallel to the  $x$ -axis for the smallest size ( $N = 2^6$ ). For large system sizes, the curves converge to different values, the larger the system size the larger the converged value. It shows that the system is in a localized state for a fixed system size. But the details of the localized states are different for different system sizes. In Fig. 1(c),  $\lambda = 2.3$ , all curves converge to a line which is parallel to the  $x$ -axis for all system sizes. So the system is in a purely localized state. Fig. 1(d) shows the curves  $P(N)$  at  $t \sim 2.0 \times 10^5$ . The inset of Fig. 1(d) shows  $\beta(\lambda)$ . When  $\lambda \lesssim 1.65$ , the system is in a purely extended state. When  $\lambda \gtrsim 1.65$ , the system becomes a semi-localized (or semi-extended) state. When  $\lambda \gtrsim 2.25$ , the system becomes a purely localized state. It seems that there is a metal-insulator transition at  $\lambda \sim 1.65$ . Figs. 2(a) - (c) show the survival probability  $P(t)$  at  $K = 0.3$ . For each  $\lambda$  and all system sizes, the curves  $P(t)$  are parallel and display a power-law behavior  $P \sim t^{-\beta}$ . In the simulation,  $\beta$  decreases from 1 to 0 as  $\lambda$  increases, and  $\beta = 0$  for  $\lambda > 3.5$ . Fig. 2(d) shows the curves  $P(N)$  at  $t \sim 2.0 \times 10^5$ . The inset of Fig. 2(d) shows  $\beta(\lambda)$ . When  $\lambda \lesssim 3.53$ , the system is in an anomalously diffused state. The diffusion exponent is a slowly decreasing function of  $\lambda$ . When  $\lambda \gtrsim 3.53$ , the system is in a purely localized state. It seems that no metal-insulator transition exists in this parameter range. The system's behavior is similar to that of the Fibonacci model.

By studying other values of  $K$ , an approximate phase diagram of the FK model is given in Fig. 3. The insets (1) and (2) show  $\beta(\lambda)$  for  $K = 0.19, 0.2$ , respectively. The line connecting the points is to guide the eyes only. From the insets, it suggests that the purely extended state will disappear at  $K \in [0.19, 2.0]$ . It suggests that there is a transition at  $K_c \in [0.19, 2.0]$ , and  $K_c$  corresponds to the critical point of the breaking of analyticity transition in the classical FK model. The phase diagram is divided into three parts: a purely localized state, an extended state, and

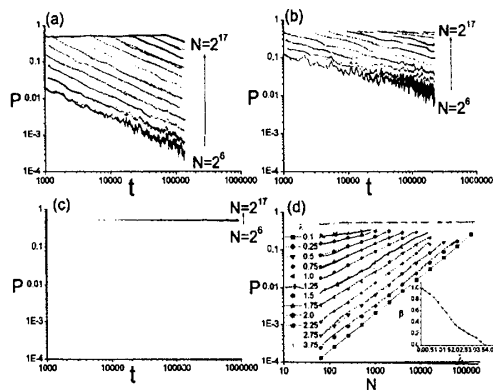


FIG. 2: Log-log plot of the survival probability  $P(t)$  at  $K = 0.3$  and various  $\lambda$  (a)  $\lambda = 0.5$ ; (b)  $\lambda = 1.5$ ; (c)  $\lambda = 3.75$ . In Fig. 2(d),  $P(N) \sim N^{-\beta}$  for different  $\lambda$  at time  $t \sim 2 \times 10^5$ . The inset of Fig. 2(d) shows  $\beta(\lambda)$ .

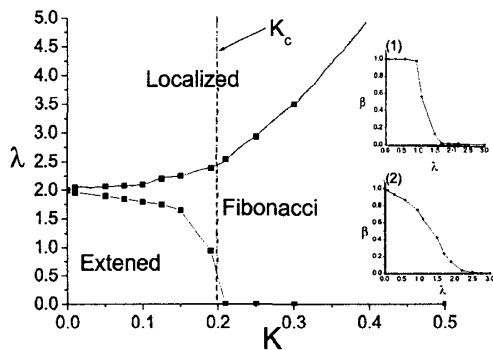


FIG. 3: An approximate phase diagram of the FK model. The insets (1) and (2) show  $\beta(\lambda)$  at  $K = 0.19$  and  $0.21$ , respectively.

a Fibonacci-like state. The curve between the extended state and Fibonacci state suggests the possible existence of a phase transition. The dotted curve between the Fibonacci state and the localized state does not imply a phase transition; it only shows that the region above the line is in the purely localized state. Therefore, in the quantum electronic FK model, the classical FK model's critical point  $K_c$  controls whether the system is Harper-like ( $K < K_c$ ) or Fibonacci-like ( $K > K_c$ ).

#### Acknowledgements

We would like to thank Drs. X. Wang, B. Li and members of the Centre for Nonlinear Studies for discussions. This work was supported in part by grants from the Hong Kong Research Grants Council (RGC) and the Hong Kong Baptist University Faculty Research Grant (FRG).

#### REFERENCES

- [1] P. G. Harper, Proc. Phys. Soc. London Sect. A **68**, 874 (1955)
- [2] S. Abe and H. Hiramoto, Phys. Rev. A. **36**, 5349 (1987); M. Dulea, M. Johansson and R. Riklund, Phys. Rev. B. **45**, 105 (1992); F. Piechon, M. Benakli and A. Jagannathan, Phys. Rev. Lett. **74**, 5248 (1995)
- [3] P. Tong, B. Li and B. Hu, Phys. Rev. Lett. **88**, 46804 (2002)
- [4] T. Geisel, R. Ketzmerick and G. Petschel, Phys. Rev. Lett. **66**, 1651 (1991)
- [5] J. Zhong, R. B. Diener, D. A. Steck, W. H. Oskay, M. G. Raizen, E. W. Plummer, Z. Zhang and Q. Niu, Phys. Rev. Lett. **86**, 2485 (2001)
- [6] R. Ketzmerick, G. Petschel and T. Geisel, Phys. Rev. Lett. **69**, 695 (1992)
- [7] A. Ossipov, M. Weiss, T. Kottos and T. Geisel, Phys. Rev. B. **64**, 224210 (2001)
- [8] A. D. Mirlin, Phys. Rep. **326**, 259 (2000); F. M. Dittes, Phys. Rep. **339**, 215 (2000)
- [9] G. Casati, G. Maspero and D. L. Shepelyansky, Phys. Rev. Lett. **82**, 524 (1999); **84**, 4088 (2000); G. Casati, I. Guarneri and G. Maspero, Phys. Rev. Lett. **84**, 63 (2000)
- [10] A. Politi, S. Ruffo and L. Tessieri, Eur. Phys. J. B. **14**, 673 (2000); M. Weiss, T. Kottos and T. Geisel, Phys. Rev. B. **63**, 81306(R) (2001)